

MEASUREMENTS OF STARSPOT AREA AND TEMPERATURE ON FIVE ACTIVE, EVOLVED STARS

DOUGLAS O'NEAL

Department of Astronomy and Astrophysics, The Pennsylvania State University, 525 Davey Laboratory, University Park, PA 16802;
oneal@astro.psu.edu

STEVEN H. SAAR

Harvard-Smithsonian Center for Astrophysics, 60 Garden Street, Cambridge, MA 02138

AND

JAMES E. NEFF

Department of Astronomy and Astrophysics, The Pennsylvania State University, 525 Davey Laboratory, University Park, PA 16802

Received 1995 August 17; accepted 1995 December 20

ABSTRACT

We present results from a study of starspot areas and temperatures on active stars using the 7055 and 8860 Å bands of the titanium oxide molecule. Because the two bands have different temperature sensitivities, the ratio of their strengths provides a measure of the spot temperature, while their absolute strengths are a function of total starspot area. We have analyzed the TiO bands of four active, evolved, single-lined spectroscopic binaries (EI Eridani, σ Geminorum, V1762 Cygni, and II Pegasi) and of the FK Comae star V1794 Cygni. Where possible, we compare our results with contemporaneous photometry, which is used to refine our estimate of the nonspotted photospheric temperature. We find that, over multiple epochs of observation, the spot filling factor ranges from below our detection threshold ($\approx 8\%$) to just under 60%. In some cases, we find that significant starspot coverage was likely present at historical light maxima. Our results suggest a possible correlation between increasing surface gravity and the temperature difference between the spotted and nonspotted photosphere. This might result from smaller starspot magnetic field strengths on active stars of lower gravity and the corresponding decrease in the pressure and temperature contrast between the photosphere and the umbra.

Subject headings: stars: activity — stars: atmospheres — stars: late-type — stars: magnetic fields — techniques: spectroscopic

1. INTRODUCTION

In a previous paper (Neff, O'Neal, & Saar 1995; hereafter Paper I), we described a technique using the absorption bands of the titanium oxide molecule at 7055 and 8860 Å to measure the effective temperatures and area coverages of starspots on active stars. We use spectra of inactive M stars to model the spotted regions of active star photospheres and spectra of inactive G and K stars to model the unspotted regions. These proxy spectra are weighted by their relative continuum fluxes and by a surface area covering factor to reproduce spectra of the active star. When these two TiO bands are measured in the spectra of active stars, the ratio of their depths is a function of the temperature of the starspots, and their absolute depths are functions of the total area of starspots on the visible hemisphere. Combining our measurements with simultaneous photometry, we are able to solve for the temperature of the unspotted photosphere. In Paper I we used this technique to determine starspot parameters for the extremely active single-lined spectroscopic binary II Peg.

Traditionally, photometric light-curve modeling has been used to measure properties of starspots (see, e.g., Strassmeier, Hall, & Henry 1994). That technique has the disadvantage that it can only measure an asymmetric spot distribution or differences from a presumed “immaculate” (unspotted) light level. A symmetric distribution, either a monolithic polar spot or smaller spots spread uniformly in longitude, will produce no variation of the star's brightness. More spatial detail can be derived using the technique of Doppler imaging, in which asymmetries in a line profile from a rapidly rotating star are used to model the asym-

metries on the stellar surface (see, e.g., Strassmeier et al. 1991; Hatzes & Vogt 1992). In contrast, our spectroscopic technique can detect starspots even on a slowly rotating star, without regard to their spatial distribution. We report the results obtained by applying the technique described in Paper I to five single-lined active stars, including further observations of II Peg.

2. OBSERVATIONS AND ANALYSIS

The data were obtained during 10 observing runs at the National Solar Observatory's McMath-Pierce Telescope. We used the stellar spectrograph system (Smith & Jaksha 1984; Smith & Giampapa 1987), including (1) a five-slice Bowen-Walraven image slicer, (2) a Milton Roy reflection grating with 1200 grooves per millimeter, used in first order, (3) a filter (Schott OG570) to remove contributions from higher orders, (4) a 105 mm Nikon transfer lens, and (5) a Texas Instruments 800 × 800 CCD (15 μm square pixels). We used a quartz lamp incident on the image slicer for flat fielding and various Th-Ar and Th-Ne lamps for wavelength calibration. We refer the reader to Paper I for details of the data reduction. The reduced spectra consist of approximately 700 medium-resolution ($\lambda/\Delta\lambda \approx 14,000$), high-S/N (200–400) spectra with a range of ~ 200 Å centered on the TiO bands beginning at 7055 Å [the 7055, 7088, and 7126 Å bands of the $\gamma(0, 0)$ system] and on the band at 8860 Å [the strongest of the $\delta(0, 0)$ system]. We observed nine dwarf and nine giant target stars, 36 inactive G and K stars, and 32 M-type comparison stars. During our 1994 February observing run we extended our original comparison star grid by adding spectra of inactive G and K

giants and of additional M giant comparison stars, primarily of higher T_{eff} than the M giants in the original comparison grid. Table 1 lists properties of the comparison stars observed in 1994 February; see Paper I for the properties of the original comparison grid. Photometry for the stars comes from Stauffer & Hartmann (1986) and the Bright Star Catalog (Hoffleit & Jaschek 1982). T_{eff} values for the M giants and cooler K giants ($T_{\text{eff}} \leq 4400$ K) were computed from the T_{eff} versus $(V-K)$ calibration of Ridgway et al. (1980); for the warmer giants, we used the T_{eff} versus $(B-V)$ calibration of Böhm-Vitense (1980). The computed T_{eff} values were rounded off to the nearest interval of 25 K. For our comparison and target stars, we define a band depth index for the 7055 Å (D_{7055}) and 8860 Å (D_{8860}) TiO bands as the difference between the pseudocontinuum flux levels (measured by averaging the five highest points in a 5 Å pass band) redward and blueward of the band head. The band depth values for the comparison stars are listed in Table 1.

In Table 2 we list the properties of the five active stars discussed in this paper. T_Q is the temperature we derive for the nonspotted regions of the star ($\geq T_{\text{eff}}$), T_S is the average temperature in the spots, V_{max} is the historical maximum V magnitude, and $V(f_S = 0)$ is the V magnitude that, based on our calculations, would be observed if the star were completely unspotted. Table 3 summarizes our observations of each active star. We list the UT date and phase of each observation, the measured depth indices for the two TiO bands, and our computed spot filling factors. On most occasions, spectra of the stars in both wavelength bands

were obtained on the same night, which is necessary to analyze short-period systems. The phases listed in Table 3 are averages of the phases of the 7055 and 8860 Å band observations, but in no case did these differ by more than $\Delta\phi = 0.03$.

Following Paper I, our analysis uses the spectra of inactive G and K stars to simulate the unspotted ("quiet") photospheres of our active target stars and spectra of M stars to simulate the spots. The normalized comparison spectra for the quiet photosphere (F_Q , with $T_{\text{eff}} = T_Q$) and the spot (F_S , $T_{\text{eff}} = T_S$) are combined to produce the model spectrum (F_{total}) using

$$F_{\text{total}} = \frac{f_S R_\lambda F_S + (1 - f_S) F_Q}{f_S R_\lambda + (1 - f_S)}, \quad (1)$$

where f_S is the total fractional projected area of spots on the observed hemisphere weighted by limb darkening (essentially the flux-weighted filling factor) and R_λ is the continuum surface flux ratio between the spot and the quiet photosphere. Our grid of inactive G/K comparison stars covers $3925 \text{ K} \lesssim T_{\text{eff}} \lesssim 5600 \text{ K}$, and our spot comparison grid, including the stars listed in Paper I, spans $3000 \text{ K} \lesssim T_{\text{eff}} \lesssim 3950 \text{ K}$.

In Paper I, we found that for $3000 \text{ K} \leq T_{\text{eff}} \leq 3800 \text{ K}$, D_{7055} and D_{8860} increase approximately linearly with decreasing T_{eff} . However, the addition of new data from M giants with $3550 \text{ K} \leq T_{\text{eff}} \leq 4000 \text{ K}$ shows that a single linear fit for each band is inadequate. For this paper, there-

TABLE 1
PROPERTIES OF ADDITIONAL COMPARISON STARS AND MEASURED BAND DEPTHS

| HD | HR | Other Names | Spectral Type | V | (B-V) | (R-I) | T_{eff} | D_{7055}^a | D_{8860}^a |
|-------------------------------------|------|--------------|---------------|-----|-------|-------|------------------|--------------|--------------|
| G and K Giant Comparison Stars | | | | | | | | | |
| 41116 | 2134 | 1 Gem | G5 III-IV | 4.2 | 0.82 | 0.45 | 5250 | ... | ... |
| 109379 | 4786 | β Crv | G5 II | 2.7 | 0.89 | 0.44 | 5050 | ... | ... |
| 82635 | 3800 | 10 LMi | G8.5 III | 4.6 | 0.92 | 0.46 | 5000 | ... | ... |
| 62345 | 2985 | κ Gem | G8 III | 3.6 | 0.93 | 0.45 | 4975 | ... | ... |
| 135722 | 5681 | δ Boo | G8 III | 3.5 | 0.95 | 0.51 | 4900 | ... | ... |
| 73593 | 3422 | 34 Lyn | G8 IV | 5.4 | 0.99 | N/A | 4825 | ... | ... |
| 76294 | 3547 | ζ Hya | G9 II-III | 3.1 | 1.00 | 0.49 | 4775 | ... | ... |
| 82734 | 3808 | ... | K0 IV | 5.0 | 1.02 | N/A | 4750 | 0.8 | ... |
| 68752 | 3229 | 20 Pup | G5 II | 5.0 | 1.07 | 0.38 | 4650 | ... | ... |
| 74442 | 3461 | δ Cnc | K0 III | 3.9 | 1.08 | 0.54 | 4625 | 1.3 | ... |
| 73471 | 3418 | σ Hya | K1 III | 4.4 | 1.21 | 0.56 | 4600 | 0.4 | ... |
| 95345 | 4291 | 58 Leo | K1 III | 4.8 | 1.16 | 0.56 | 4600 | 1.5 | ... |
| 66216 | 3149 | χ Gem | K2 III | 4.9 | 1.12 | N/A | 4525 | 2.6 | ... |
| 81146 | 3731 | κ Leo | K2 III | 4.5 | 1.23 | 0.63 | 4350 | 1.3 | ... |
| 127665 | 5429 | ρ Boo | K3 III | 3.6 | 1.30 | 0.65 | 4300 | 2.3 | ... |
| 98262 | 4377 | ν UMa | K3 III | 3.5 | 1.40 | 0.70 | 4200 | 3.5 | ... |
| 69267 | 3249 | β Cnc | K4 III | 3.5 | 1.48 | 0.78 | 4050 | 1.9 | ... |
| 70272 | 3275 | 31 Lyn | K4.5 III | 4.3 | 1.55 | 0.88 | 3950 | 9.9 | ... |
| 120477 | 5200 | ν Boo | K5.5 III | 4.1 | 1.52 | 0.87 | 3950 | 13.5 | 1.7 |
| 80493 | 3705 | α Lyn | K7 III | 3.2 | 1.55 | 0.90 | 3925 | 11.6 | 0.8 |
| Additional M Giant Comparison Stars | | | | | | | | | |
| 116870 | 5064 | 68 Vir | M0 III | 5.3 | 1.52 | 0.87 | 3950 | 11.6 | 1.1 |
| 89758 | 4069 | μ UMa | M0 III | 3.1 | 1.59 | 0.96 | 3950 | 18.3 | 2.2 |
| 60522 | 2905 | ν Gem | M0 III | 4.1 | 1.54 | 0.91 | 3925 | 15.5 | 2.2 |
| 129712 | 5490 | 34 Boo | M3 III | 4.8 | 1.66 | 1.22 | 3700 | 35.0 | 5.4 |
| 55383 | 2717 | 51 Gem | M4 III | 5.0 | 1.66 | 1.25 | 3700 | 43.8 | 14.1 |
| 112142 | 4902 | ψ Vir | M3 III | 4.8 | 1.60 | 1.28 | 3650 | 37.3 | 6.1 |
| 112300 | 4910 | δ Vir | M3 III | 3.4 | 1.58 | 1.33 | 3650 | 42.5 | 8.8 |
| 29755 | 1496 | 54 Eri | M3-4 III | 4.3 | 1.61 | 1.38 | 3625 | 43.1 | 8.5 |
| 40239 | 2091 | π Aur | M3 II | 4.3 | 1.72 | 1.48 | 3600 | 44.8 | 11.0 |
| 19058 | 921 | ρ Per | M4 II | 3.4 | 1.65 | 1.62 | 3550 | 51.9 | 17.8 |

^a Band depth index, in percent of continuum level.

1996ApJ...463..766O

TABLE 2
PROPERTIES OF ACTIVE STARS

| Parameter | EI Eri | V1794 Cyg | σ Gem | V1762 Cyg | II Peg |
|-------------------------------|---------------------------|----------------------------|---------------------------|----------------------------|---------------------------|
| HD..... | 26337 | 199178 | 62044 | 179094 | 224085 |
| Spectral type..... | G5 IV | G5 III | K1 III | K1 III-IV | K2 IV-V |
| P_{rot} (days)..... | 1.945 ^a | 3.337484 ^b | 19.60447 ^c | 28.5895 ^d | 6.72442 ^e |
| HJD for $\phi = 0$ | 2,444,635.65 ^a | 2,444,395.780 ^b | 2,447,227.08 ^c | 2,442,479.214 ^d | 2,443,033.47 ^e |
| $\log g$ | 3.8 | 3.3 | 2.5 | 3.2 | 3.7 |
| T_{eff}^f | 5600 K | 5350 K | 4500 K | 4550 K | 4800 K |
| T_{S}^f | 3700 K | 3800 K | 3850 K | 3450 K | 3500 K |
| V_{max}^g | 6.96 ^g | 7.16 ^b | 4.14 ^g | 5.74 ^c | 7.2 ^g |
| $V(f_{\text{S}} = 0)^g$ | ... | 6.9 | 4.14 | 5.75 | 6.8 |

^a Strassmeier 1990.

^b Jetsu et al. 1990.

^c Bopp & Dempsey 1989.

^d Strassmeier, Hall, & Henry 1994.

^e Vogt 1981.

^f Our TiO results.

^g Strassmeier et al. 1993.

fore, we use multiple linear fits to better approximate the band depth versus T_{eff} relations (see Fig. 1). For the 7055 Å band, the shallower slope of the relation toward lower T_{eff} is likely due to the absorption beginning to saturate. The multiple fit to the 8860 Å band depth is necessary because the band is almost twice as strong in M4 III stars than in M3 III stars at only slightly lower T_{eff} . We fitted D_{7055} with a two-piece linear fit:

$$D_{7055} = \begin{cases} -0.3836 \frac{T_{\text{eff}}}{1000 \text{ K}} + 1.855, & 3000 \text{ K} \leq T_{\text{eff}} \leq 3575 \text{ K}, \\ -0.9226 \frac{T_{\text{eff}}}{1000 \text{ K}} + 3.773, & 3575 \text{ K} < T_{\text{eff}} \leq 4000 \text{ K}. \end{cases} \quad (2)$$

We fitted D_{8860} with a discontinuous two-piece linear fit:

$$D_{8860} = \begin{cases} -0.6337 \frac{T_{\text{eff}}}{1000 \text{ K}} + 2.423, & 3000 \text{ K} \leq T_{\text{eff}} \leq 3575 \text{ K}, \\ -0.2522 \frac{T_{\text{eff}}}{1000 \text{ K}} + 1.009, & 3575 \text{ K} < T_{\text{eff}} \leq 4000 \text{ K}. \end{cases} \quad (3)$$

Figure 2 shows the 7055 Å band versus T_{eff} relation in the warmer stars, illustrating the markedly different behavior of

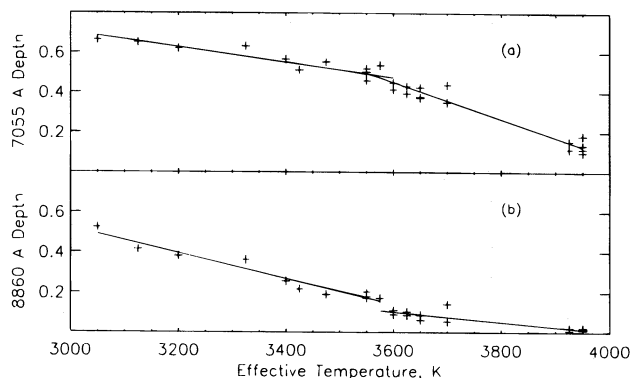


FIG. 1.—(a) Plot of 7055 Å band depth vs. T_{eff} for M giant comparison stars. (b) Plot of 8860 Å band depth vs. T_{eff} for M giant comparison stars. The best-fit multilinear relationships are overplotted.

dwarfs and giants. The depths increase from below our sensitivity limit ($\approx 0.5\%$) for $T_{\text{eff}} \geq 4600$ K, to $\sim 3\%$ at 4100 K. The absorption strengths for both classes of stars rise rapidly for $T_{\text{eff}} \leq 4000$ K, but D_{7055} in giants increases much more quickly with decreasing T_{eff} .

Another significant change in our method since Paper I involves the way we have computed R_{λ} , the ratio of spot continuum flux to nonspot continuum flux. We use models by Kurucz (1991) for the value of $\log g$ appropriate to each active star, giving flux values averaged over 20 Å band passes just blueward of the 7055 and 8860 Å band heads. Those models are not computed for $T_{\text{eff}} < 3500$ K, so we extrapolated to lower T_{eff} using the models by Allard (1990). Originally, we approximated the relationship between $\log(T_{\text{eff}})$ and $\log(\langle F \rangle)$ with a quadratic fit. These fits underestimated R_{λ} for some T_{eff} values, leading us to overestimate the f_{S} needed to produce a given D . Here we have replaced these quadratic fits by linear spline fits, which allow better interpolation for intermediate values. Our revised f_{S} values for the 1989 October II Peg data are smaller by ≈ 0.1 than the values given in Paper I.

Uncertainties in our determination of f_{S} for an active star result from uncertainties in both the linear fits to the band depths of M giant stars and the depth measurements themselves. The depth of the 8860 Å band on active stars is

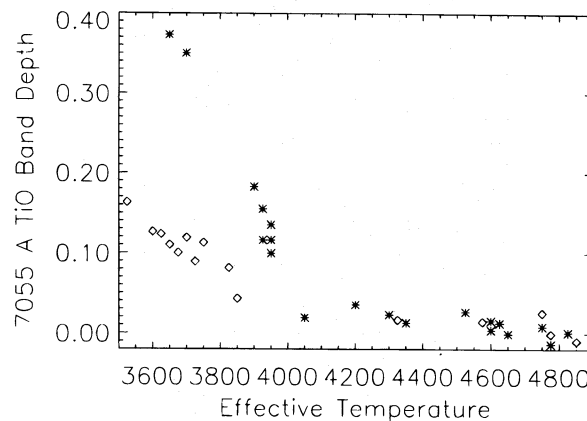


FIG. 2.—Behavior of the 7055 Å TiO band depth against temperature for K stars and early M stars. Asterisks denote giants, diamonds denote dwarfs. Above $T_{\text{eff}} = 4000$ K the behavior is similar. Below 4000 K, the absorption in giants increases much more rapidly with decreasing temperature.

generally less than 4% of the continuum, and D_{7055} ranges from 1% to 6%. We can get an idea of the uncertainty in our depth measurements by studying spectra of stars with no TiO absorption, i.e., stars with $T_{\text{eff}} > 4800$ K. Applying our band depth definition to such spectra, we find that the mean of the "depth" signal for these spectra is $\pm 0.5\%$ in each band. A purely statistical calculation that takes the rms deviation of the difference between the averages of two sets of five points presumed to have intensity values of 1, with $S/N \approx 200$, gives $\delta D = \pm 0.3\%$. Because of systematic errors in our method, such as the many blended and unresolved atomic lines in cool star spectra, we take the higher, empirical value as the uncertainty in measuring a molecular band depth by our technique.

Intrinsic variability of the band depths in M giant stars (discussed further in § 4.3) is larger than the measurement error. Each depth value listed in Table 1 is an average of depth values measured from two to four observations of each star. Given this small number of observations, we have very little information about the intrinsic scatter of the points plotted in Figure 1. Instead, we use the standard deviations of each of the linear fits (0.033 for the D_{7055} fit and 0.032 for D_{8860}) as the combined variability plus intrinsic uncertainty in D . We can then propagate these uncertainties through equation (1) to compute the uncertainty in f_S .

For this calculation, we simplify equation (1) by considering the measured flux level in the active star spectrum redward of the band head, $F_r = 1 - D_{\text{active}}$. We further take $F_Q = 1$, and $F_S = 1 - D_S$, the depth of the TiO band in the starspot proxy being used. Then we have

$$f_S = \frac{F_r - 1}{(R_\lambda)(1 - D_S - F_r^{-1}) + F_r - 1}. \quad (4)$$

We use equation (4) to compute the uncertainty δf_S for given values of f_S , which depends upon D_S (equivalently T_S), F_r , and R_λ (equivalently T_Q , after T_S is fixed).

Figure 3 presents δf_S as a function of f_S for two pairs of assumed temperature values: (Fig. 3a) $T_S = 3500$ K, $T_Q = 4800$ K; and (Fig. 3b) $T_S = 3600$ K, $T_Q = 5400$ K. The uncertainty, especially that derived from D_{8860} , rises appreciably when both T_S and T_Q rise due to the shallower TiO band in the spot spectrum and to the lesser effect of the spot on the overall continuum of the star (a lower R_λ).

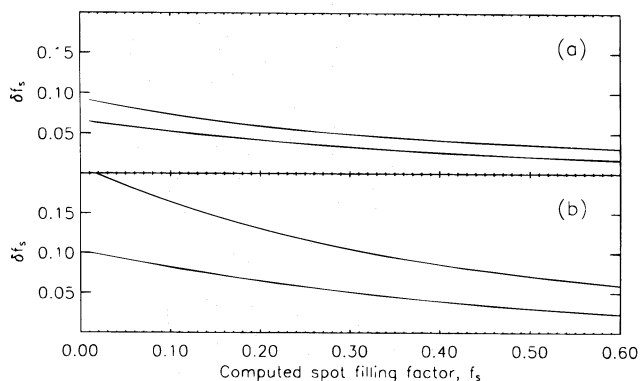


FIG. 3.—The uncertainty, δf_S , in our calculation of spot filling factor as a function of f_S for two pairs of temperature values: (a) $T_Q = 4800$ K and $T_S = 3500$ K; and (b) $T_Q = 5400$ K and $T_S = 3600$ K. In each plot, the upper curve represents δf_S if f_S is derived solely from the active star's D_{8860} , while the lower curve represents δf_S when f_S is computed from only D_{7055} .

We can also estimate the error in T_S due to the uncertainty in measuring the band depths. T_S is computed from the ratio of the depths of the two bands in active stars; for active stars with strong bands, such as II Peg, $\delta T_S \approx \pm 100$ K; for stars with smaller f_S and $T_S \approx 3800$ K, δT_S can be as high as 250 K.

3. RESULTS

3.1. *EI Eri* (=HD 26337)

EI Eri is a noneclipsing, single-lined spectroscopic binary with a period of 1.95 days, and $v \sin i = 50 \text{ km s}^{-1}$. It has a G5 IV spectral type, and Strassmeier et al. (1991) assume an effective temperature of the unspotted regions of 5500 K. Fekel et al. (1987) estimate $1.4 \leq M/M_\odot \leq 1.8$ and $R \sin i \approx 1.9 R_\odot$ with $i = 46^\circ \pm 12^\circ$. Based on these values, we take $M/M_\odot \approx 1.6$ and $R/R_\odot \approx 2.6$, yielding $\log g \approx 3.8$ (consistent with $\log g = 3.75$ used by Hackman et al. 1991). We used the $\log g = 4.0$ Kurucz models.

Strassmeier (1990) finds a spot temperature of 3600 ± 400 K, agreeing with the measurement by Hatzes & Vogt (1992). The best fit to the light curve of EI Eri in both studies was obtained with an asymmetric polar spot and up to three spots at low latitudes. Strassmeier (1990), using photometry, derives spot areas varying from 6.4% to 10.3%.

We find a similar value for T_S , 3700 ± 200 K, but substantially higher f_S , varying from 16% to 37% among three different epochs (Table 3). On 1989 October 9, 11, and 13, respectively, we determined $f_S = 17\%$, 22% , and 27% ; because $P_{\text{rot}} \approx 2$ days, these measurements were at practically the same rotational phase. An October 14 observation of the opposite hemisphere yielded $f_S = 20\%$. Given our experimental uncertainty, the differences in f_S from the first three observations are only barely significant. It is possible, however, that they indicate a growing or erupting spotted region on one hemisphere. To illustrate the excess 7055 Å TiO band absorption typical of heavily spotted stars, Figure 4 compares a spectrum of EI Eri (obtained 1990 March 18, at maximum f_S) with an artificially rotationally broadened spectrum of 61 UMa, an inactive star of similar T_{eff} .

The published photometry for EI Eri closest to our 1989 October observations is that of Rodonò & Cutispoto (1992) from late 1989 November. They use an older ephemeris

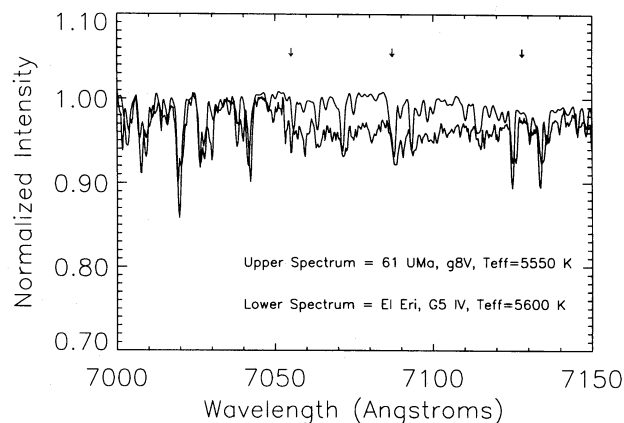


FIG. 4.—A comparison of a spectrum of the active star EI Eri, $T_{\text{eff}} = 5600$ K, with an artificially rotationally broadened spectrum of the inactive star 61 UMa, $T_{\text{eff}} = 5550$ K. Positions of the three TiO bands are marked with arrows. Excess absorption due to the spottedness of EI Eri is evident.

(Fekel et al. 1987); to compare our results with their observations, we must subtract 0.13 from their phases. Photometric minimum was between phase 0.35 and 0.40, and the star was 0.06 mag dimmer in the V band at phase 0.53 (which we observed on October 9, 11, and 13) than at phase 0.05 (October 14). If our three observations of phase 0.53 are averaged, we find a slightly greater spot coverage at phase 0.53 than at phase 0.05. This may not be a meaningful comparison, however, because 5 weeks separate the photometry from our spectroscopy, and the light curve can change radically within this span of time (e.g., Strassmeier 1990). The $\langle B-V \rangle = 0.67$ (Rodonò & Cutispoto 1992; Strassmeier et al. 1993) is better fitted with $T_Q = 5600$, so we have used this value in computing f_S . Since we do not have photometry contemporaneous with our TiO observations, we do not calculate $V(f_S = 0)$ for EI Eri.

3.2. V1794 Cyg (= HD 199178)

V1794 Cyg is an FK Comae variable, a rapidly rotating ($v \sin i = 73 \text{ km s}^{-1}$; Dempsey et al. 1992) single star that might be the product of the coalescence of a binary system (Huenemoerder 1986). Its light curve is stable on timescales of ~ 1 month, and its $(B-V)$ color varies in phase with its V magnitude (Rodonò & Cutispoto 1992), indicating the presence of starspots. Its period is 3.337 days and $i = 82^\circ$. The star's G5 III or III-IV spectral type implies $T_{\text{eff}} \approx 5400 \text{ K}$ (Jetsu et al. 1990) and $3.0 \lesssim \log g \lesssim 3.5$ (Gray 1988); we take $\log g \approx 3.3$.

Jetsu et al. (1990) find $\Delta T \equiv T_Q - T_S = 580 \pm 105 \text{ K}$; some of their individual data sets are best fitted with values up to 1240 K, but with larger errors. The maximum f_S for various models ranged from 9% to 45%, 25% being the value if the "best" spot temperature is assumed. Dempsey et al. (1992) find a polar spot whose shape and area can vary on short timescales.

The 8860 Å TiO band head was too weak to detect in spectra of V1794 Cyg. While this eliminates one of the constraints on T_S and f_S , we can nonetheless set limits on these parameters. The detection of the 7055 Å band indicates a significant f_S , and $D_{8860} \approx 0$ implies $T_S \geq 3800 \text{ K}$, the T_S at which the 8860 Å band would first be detectable in an active star spectrum. Since $D_{7055} \lesssim 3\%$ for stars with $T_{\text{eff}} \geq 4000 \text{ K}$, and we observe $0.8\% \leq D_{7055} \leq 2.3\%$ on V1794 Cyg, $T_S \lesssim 4000 \text{ K}$ to avoid unreasonably large f_S values. Due to the rapidly changing value of D_{7055} in this temperature region, increasing T_S from 3800 K to 3900 K increases computed f_S values by ~ 0.06 , while increasing T_S to 4000 K raises f_S a further 0.1. With initial estimates of $T_Q = 5400 \text{ K}$ and $T_S = 3900 \text{ K}$, we computed f_S values for each observation.

Analysis of contemporaneous photometry was used to refine the spot parameters. The photometry for 1989 October comes from Jetsu et al. (1990) and from Dempsey et al. (1992). L. Jetsu (private communication) supplied unpublished photometry of V1794 Cyg from 1992 September. We generated synthetic photometry by constructing model spectra from weighted sums of Kurucz models ($\log g = 3.5$) using equation (1), the assumed values of T_S , and T_Q , and f_S derived from TiO bands. These model spectra were convolved with the appropriate photometric filter response functions to yield $(B-V)_{\text{Kurucz}}$. To reduce possible calibration problems with the synthetic photometry, we transformed this $(B-V)_{\text{Kurucz}}$ to a theoretical T_{eff} using the $(B-V)_{\text{Kurucz}}$ versus T_{eff} (Kurucz) relation implied

by the run of models. This T_{eff} (Kurucz) was then substituted into an empirical T_{eff} versus $(B-V)$ (see § 2) to derive the "observational" $(B-V)$ used for comparison with published photometry. By this circuitous calibration procedure, we hope to reduce any systematic errors between synthetic and observed photometric color versus T_{eff} calibrations.

With the original T_Q and T_S estimates, the synthetic photometry predicted too large a V -band brightness change (0.2 rather than the observed 0.15) and a $(B-V)$ color that was slightly too blue (by ~ 0.02). By adjusting T_Q and T_S , we eventually found excellent agreement between photometry and TiO estimates for $T_Q = 5350 \text{ K}$, $T_S = 3800 \text{ K}$, and $16\% \leq f_S \leq 32\%$ (1989 October 9–13) and $23\% \leq f_S \leq 37\%$ (1992 September 12–16). Analysis of the photometry yields an average of 7% less spot coverage than that derived from TiO bands; the TiO values are given in Table 3. Using our f_S values, the "immaculate" star, with no spot coverage, would have $V(f_S = 0) \approx 6.9$, compared with $V(f_S = 0) = 7.16$ (Jetsu et al. 1990). Vogt (1988) presents a Doppler image of the star including a polar spot, which would produce no rotational modulation.

Figure 5 displays the computed starspot coverages for V1794 Cyg as a function of phase during 1989 October and 1992 September. Spot maximum in late 1989 was near $\phi = 0.6$, in agreement with the light minimum at that phase (Dempsey et al. 1992). Our observations were obtained shortly after a large longitude/phase shift in the location of the inhomogeneous spot component. This phase shift may indicate a photometric "flip flop," similar to that detected in another star of this type, FK Comae Berenices (Jetsu, Pelt, & Tuominen 1993). Our 1992 September 11–16 data agree qualitatively with the photometry supplied by Jetsu, which shows photometric minimum still near phase 0.6 and maximum around phase 0.2.

3.3. σ Gem (= HD 62044)

Strassmeier et al. (1988) give $T_{\text{eff}} = 4400 \text{ K}$ for this K1 III star. Its period is 19.4 days, and $v \sin i = 25 \text{ km s}^{-1}$. Measured T_S values have ranged from 3400 K (Henry et al. 1995; Dempsey et al. 1992) to 3870 K (Strassmeier et al. 1988; Olah et al. 1989). From tables in Gray (1988), we estimate $\log g \approx 2.5$. Hatzes (1993), in a Doppler imaging analysis, uses $T_S = 3850 \text{ K}$ and finds several spots near but not strad-

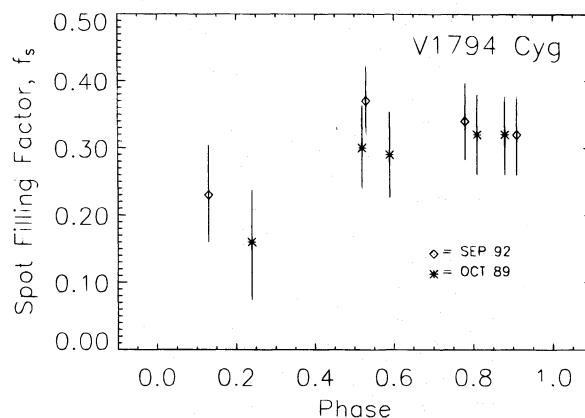


FIG. 5.—Spot filling factors for V1794 Cyg as a function of rotational phase. Asterisks denote observations in 1989 October, diamonds denote observations in 1992 September. These calculations assume $T_Q = 5350 \text{ K}$ and $T_S = 3800 \text{ K}$.

dling the pole. Strassmeier et al. (1988) found a spot coverage varying from 4% to 12%.

The 8860 Å band depth was too weak to be measured in σ Gem; thus $T_s \geq 3800$ K. A K1 giant may be cool enough so that the unspotted photosphere exhibits measurable 7055 Å band TiO absorption. We observed two inactive stars of spectral type K1 III: σ Hya and 58 Leo. Our observations reveal a mean 7055 Å depth of 1.0%. This must be taken into account when computing f_s for σ Gem. However, on two dates in 1989 March, we measured no 7055 Å band absorption. These observations fall within the broad photometric maximum found by Dempsey et al. (1993) during the 1988–1989 observing season (they use a different ephemeris, so our 1989 March observations correspond to their phases 0.88 and 0.98). These two observations also occur near the phase where spot N of Henry et al. (1995) would be approaching the subobserver longitude on the star; during this time, spot N had gone into temporary “remission” and had no effect on the star’s light curve. The lack of 7055 Å band TiO absorption in 1989 March suggests $T_Q > 4600$ K, the T_{eff} at which giant stars in our comparison grid begin to show a measurable D_{7055} . This is contrary to both Strassmeier et al. (1988) and to simultaneous photometry. An inspection of the 1989 March 12 7055 Å region spectrum reveals that the atomic lines are “filled in” relative to other spectra of σ Gem, a possible indication of a flare; the equivalent widths of these lines are as much as 50% less than the equivalent widths of the same lines on other nights. Simultaneously, Henry et al. (1995) observed $(B-V) = 1.098$, rather than the typical value of 1.12. The same anomaly may have affected the spectrum from 2 days earlier and given the illusion of no 7055 Å TiO absorption strength.

In an effort to better define T_Q , we use photometry provided by Henry et al. (1995). Using the synthetic photometry procedure outlined in § 3.2, we find that we can fit the $(B-V)$ colors and the V variations of σ Gem with $T_Q = 4500$ K and $T_s = 3850$ K. Using these values and $D_{7055} = 1.0\%$ in the quiet photosphere, we compute the f_s values (Table 3). Our combined analysis of the TiO bands and photometry imply that the immaculate star has $V(f_s = 0) \approx 4.14$, consistent with the brightest V ever observed (Strassmeier et al. 1993). Photometric and TiO f_s values agree to within 4%, on average.

Due to the long rotation period of this star, our observations in no case cover a substantial fraction of a period. However, comparisons are possible between our spectroscopic data and published photometric analyses. Figure 6 presents f_s as a function of phase for our observations of σ Gem. Our first observation during 1988 March was near in phase to “spot B” seen by Olah et al. (1989). The shape of the light curve of σ Gem can change appreciably from year to year, and by the spring of 1990 (Dempsey et al. 1992) phase 0.8 was near the photometric minimum. Our 1990 March observations covered the phases of photometric maximum, from phases 0.95 to 0.10 by the ephemeris used by Dempsey et al. (1992). We find $f_s = 14\%$ – 19% for these dates. For our observations of 1990 April, which occurred near in phase to “spot B” of Dempsey et al. (1992), we compute $f_s = 23\%$ – 26% . Our observations of 1990 December and 1991 February would have seen spots N and O of Henry et al. (1995) ~ 0.15 and 0.1 rotation, respectively, short of the star’s central meridian. Based on our data, f_s was much greater for 1991 February 6 than for 1990 December 17, perhaps due to both spot O’s larger size

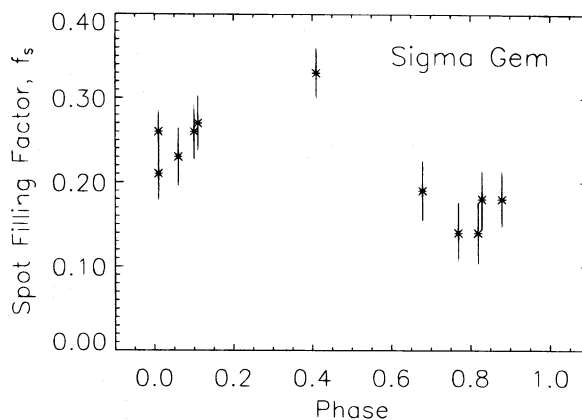


FIG. 6.—Spot filling factors for σ Gem as a function of rotational phase. These calculations assume $T_Q = 4500$ K and $T_s = 3850$ K.

during this period and of its position closer to the center of the visible hemisphere during our observation. Finally, our observation of 1994 February revealed $f_s = 27\%$.

3.4. V1762 Cyg (=HD 179094)

A K1 subgiant in an RS CVn binary, V1762 Cyg has a 28.6 day period. The shape of its light curve is variable, as is the strength of its filled-in H α absorption. Strassmeier et al. (1994) give $T_{\text{eff}} = 4820$ K and detect 20 individual spots in 15 yr of V -band photometry. Their best value for ΔT is 800 K, although Poe & Eaton (1983) favored $\Delta T = 1200$ K. The largest spot coverage found by Strassmeier et al. (1994) was 17.4%. Schrijver & Zwaan (1991) estimate $M/M_\odot \approx 2$ and $R/R_\odot \approx 6$, so $\log g \approx 3.2$.

We obtained one pair of spectra of V1762 Cyg, on 1989 March 12. Our observation was at phase 0.04, near photometric minimum for 1988–1989 (Strassmeier et al. 1994). Maximum brightness in that epoch (when $\Delta V \approx 0.2$) was ≈ 0.15 mag fainter than the brightest V magnitude ever recorded for the star, implying a substantial symmetric component to the starspot coverage. Initially assuming $T_Q = 4800$ K, our spectra were best fitted with $T_s = 3600$ K and $f_s = 35\%$. Synthetic photometry using the Kurucz models and these values, however, predicts $(B-V) = 0.99$, which is much too blue, since $\langle B-V \rangle = 1.09$ (Strassmeier et al. 1993) and our observation took place near maximum f_s and $(B-V)$. If all the TiO absorption is due to the spots, we find good agreement with both TiO and photometry for $T_Q = 4550$ K, $T_s = 3600$ K, and $f_s = 31\%$, yielding $V(f_s = 0) \approx 5.66$ for the unspotted star.

Since T_Q is so cool, though, we need to consider possible contributions to the TiO absorption from the quiet regions. The K1 IV star HR 3808 ($T_{\text{eff}} = 4750$ K) shows $D_{7055} = 0.8\%$. Giant stars at 4600 K are just beginning to show measurable D_{7055} , and presumably subgiants behave similarly. The best fit assuming a 1% 7055 Å band depth from the unspotted photosphere is $T_Q = 4550$ K, $T_s = 3450$ K, and $f_s = 24\%$. These values imply that the actual unspotted star has $V(f_s = 0) \approx 5.75$, consistent with the historical maximum $V_{\text{max}} \approx 5.74$ (Strassmeier et al. 1993). We have adopted this result as our “best solution.”

3.5. II Peg (=HD 224085)

In Paper I we presented TiO band spectroscopy of II Peg taken in 1989 October. Using the new R_λ values and band

depth versus T_{eff} relations, and assuming $T_Q = 4800$ K, we compute f_S between 43% and 55% and $T_S = 3500 \pm 100$ K for those data. We also observed II Peg from 1992 September 11 to 16 (missing September 13 due to clouds) and derive similar f_S and T_S for that epoch. Figure 7 presents our computed f_S values for both epochs.

Henry et al. (1995) present photometric spot models for II Peg covering 1973–1992. In 1989 October we would have observed their spots J and K, while spot L had the greatest effect on the light curve by 1992 September. We measure large starspot filling factors even at phases where none of the spots are centrally located on the disk; thus there must be a substantial symmetric spotted component on II Peg, in the form of either a polar spot or smaller spots evenly distributed in longitude.

As in Paper I, we had difficulty bringing photometric and TiO results into agreement. If only the changes in ΔV and $(B - V)$ are considered, we can fit the data with $T_Q = 4800$ and $T_S = 3500$, which produces a difference between f_S values derived from photometry and TiO of 6%. As noted in Paper I, however, the contemporaneous *BVRI* photometry for the 1989 data set yields a 23% greater spot coverage than we calculate from TiO. We suspect that the reason for this discrepancy is that we have used M giant spectra as spot proxies for the subgiant II Peg; the *R* and *I* bands, which accentuate the spot contribution, highlight this problem better than the *B* and *V* bands. Using our TiO results and contemporaneous photometry, we calculate $V(f_S = 0) = 6.8$, compared to $V_{\text{max}} = 7.2$ (Strassmeier et al. 1993).

Byrne et al. (1995) derived a three-spot model of II Peg in which the spots have different temperatures: a $T_S = 3600$ K spot covering 4.1% of the star's surface, a $T_S = 3200$ K spot covering 1.4% of the star, and a 2600 K spot covering 3.3% of the star. They also note that at least 20% of the star was covered by a symmetric spot distribution, for which they do not give T_S . The two cooler spots, if also present during our observations, would contribute negligibly to the overall TiO band depths, due to their small f_S and R_λ compared to the symmetric spot distribution. Our method cannot as yet detect the presence of more than one T_S on a star in the same epoch. Also, we have not yet observed T_S to vary between epochs on any of our target stars.

The companion of II Peg has never been detected. Doyle et al. (1992) hypothesize that a photometric "dip" they

observe at $\phi = 0$ could be due to an eclipse by an M0 dwarf with $R \approx 1 R_\odot$, compared to the primary's $R = 2.8 R_\odot$. If a companion of this type were present, its TiO bands would mimic only a small f_S . Assuming parameters for the M dwarf based on those given for our dwarf proxy stars in Paper I, the combined light from this secondary and an unspotted primary of $T_{\text{eff}} = 4800$ K would exhibit only $D_{7055} = 0.003$ and $D_{8860} = 0.001$, less than our measurement uncertainty. Assuming $T_Q = 4800$ K, $T_S = 3500$ K, $f_S = 40\%$, and an M0 $1 R_\odot$ companion, we would derive $f_S = 43\%$. In reality, $R \approx 1 R_\odot$ is unrealistically large for an M0 dwarf; Gray (1988) gives $R = 0.54 R_\odot$. Thus the actual effect of the secondary on the TiO-band spectra of II Peg would be considerably less than this calculation indicates.

4. DISCUSSION

4.1. Effects of Changing T_Q and T_S

When we compute f_S and T_S for a given active star, if we change the presumed T_Q value by 100 K, f_S changes in the same direction by 1.5%–2%, but T_S is unaltered. A hotter photosphere contributes more light to the overall spectrum and dilutes the contribution from the spot, forcing a larger f_S value to match the observed band depths. The relationship, for a given band, between the best-fit T_S and f_S depends on whether changes in band depth or continuum level dominate as T_{eff} is varied. If T_S is increased by 50 K, f_S computed from D_{8860} increases by an average of 2%–3%. A warmer spot exhibits weaker TiO absorption, requiring a larger f_S to reproduce the same D_{8860} . However, when f_S is computed from D_{7055} , a 50 K warmer spot requires $\sim 1\%$ less spot coverage to reproduce the same band depth. This arises because the warmer spot has a brighter continuum and contributes more to the total flux from the star at 7055 Å than a cooler spot, more than compensating for the cooler spot's greater intrinsic D_{7055} .

4.2. Effects of Gravity

For a given T_{eff} , the 8860 Å band is ~ 5 times weaker in M dwarfs than in M giants, and the 7055 Å band is about half as strong. Because of this, neither II Peg (see also Paper I) nor V1762 Cyg can be fitted with M dwarf starspot proxies. Using dwarf proxies, even very cool spots cannot account for D_{8860} in these stars, since while lower T_S increases the intrinsic band depths, R_λ shrinks even faster, making the resulting TiO bands nearly invisible against the bright photosphere. Giant stars are not ideal either for modeling active subgiants, but for the giant stars V1794 Cyg and σ Gem we were able to achieve quite good agreement between TiO and results based on contemporaneous photometry, with the average difference in f_S values derived from TiO and photometry of less than 7%.

It has been suggested that starspots should be represented by lower gravity models than the surrounding photosphere. If P_{ext} and P_{int} are the gas pressures external and internal to the spot, then $P_{\text{int}} \approx P_{\text{ext}} - B_S^2/8\pi$, where B_S is the spot field strength. The spot atmosphere has a lower pressure and thus a lower effective gravity than the quiet photosphere surrounding it. This equation holds for force balance at equal *geometric* heights. It is more important spectroscopically, however, to compare equal *optical depths*, since the latter will define where the TiO bands and other spectral features are formed. When umbral core and photospheric models are compared at equal τ surfaces (see, e.g.,

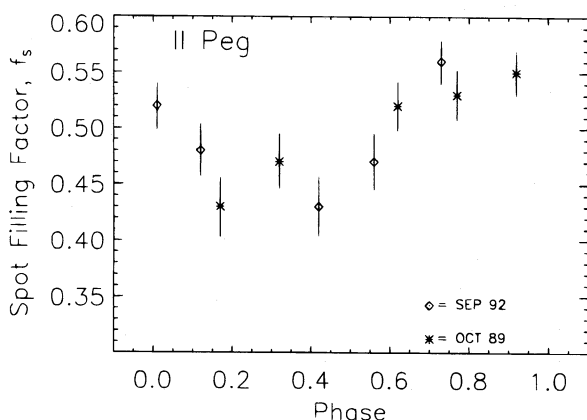


FIG. 7.—Spot filling factors for II Peg as a function of phase. Asterisks denote observations in 1989 October, diamonds observations in 1992 September. These calculations assume $T_Q = 4800$ K and $T_S = 3500$ K.

Maltby et al. 1986), $P_{\text{int}}(\tau_{0.5})$ is actually slightly higher than $P_{\text{ext}}(\tau_{0.5})$. Thus, lower gravity models are *not* appropriate for starspots that are similar to solar umbrae in structure.

The f_s values can also change if different $\log g$ model atmospheres are used to compute R_λ . For instance, given a star with $T_s = 3500$ K and $T_Q = 4800$ K, R_λ at 7055 Å decreases from 0.148 at $\log g = 4$ to 0.107 at $\log g = 3$. R_λ at 8860 Å also decreases, from 0.260 to 0.223. This change does not affect the T_s that we compute from both D_{7055} and D_{8860} , but it does increase the f_s needed to reproduce the observed band depths. For a $\log g = 4$ star on which we observed $D_{7055} = 0.05$ and $D_{8860} = 0.03$, we would calculate $f_s = 41\%$; decreasing $\log g$ to 3, however, would increase f_s to 46%. Likewise, if $D_{7055} = 0.02$ and $D_{8860} = 0.012$, decreasing $\log g$ from 4 to 3 increases f_s from 21% to 24%.

4.3. Variability of M Giant Band Depths

In both Paper I and this paper, we present linear fits to the relations between T_{eff} and measured TiO band depths in M giant stars. Many of the M giants are variable stars, and we need to ascertain to what extent D_{7055} and D_{8860} in those stars are intrinsically variable.

Of the 23 M giant comparison stars presented in Paper I and here, we have multiple 7055 Å band observations of 19 of the stars, and multiple 8860 Å band observations of 18. Using χ^2 analysis and the 0.005 uncertainty in measuring band depths, we find that 11 M giants exhibit almost certainly ($>99.9\%$ probability) variable D_{7055} . Six of these 11 stars are almost certainly variable in D_{8860} as well, but five others have a high statistical likelihood of being constant. In five of six cases where we have observations of one star in both wavelength bands from two different observing runs and where the strengths of both bands varied between the runs, they varied in the same manner, i.e., both increased or both decreased. For this limited data set, there is no apparent correlation between ΔD_{7055} and ΔD_{8860} .

None of the band depths of M giant stars observed only in 1994 February have greater than a 90% probability of being variable. This is likely due to two effects. First, the variability timescales in M giants tend to be much longer than our 5 day observing window. Also, cooler M giants tend to be more variable (e.g., Feast 1981), and the 1994 observations were of mostly warmer ($T_{\text{eff}} > 3550$ K) stars. Consistent with this, the only two members of the original M giant list whose 7055 Å depths are not definitely variable, μ Gem and τ^4 Eri, are two of the three warmest M giants observed for Paper I. Given our limited number of observations, it is not possible to estimate the true variability of the band depths, but since $T_s \geq 3500$ K for all the active stars we discuss here, intrinsic variability of the cooler M giants only minimally affects our TiO modeling of active stars.

4.4. Computed Spot Filling Factors

In some cases, notably EI Eri, our computed spot coverages are substantially greater than coverages found by photometry and Doppler imaging techniques. For instance, Strassmeier (1990) found a maximum 10.3% spot coverage for EI Eri, compared to our maximum f_s of 37%. Our spectroscopic method can detect uniform spot distributions, which are difficult to detect photometrically, just as easily as it detects asymmetrically distributed spots. Many investiga-

tors model starspot distributions with a small number of very large spots or spot groups on otherwise pristine stars. Differences between the maximum V at the modeled epoch and the historic maximum are accounted for by a polar spot, which yields no rotational modulation. Our TiO results imply that the true spot coverage can be substantially higher than that found by light-curve modeling. We have used our computed spot parameters to estimate the V magnitude for the pristine stars [$V(f_s = 0)$; Table 2]. For V1794 Cyg and II Peg, these values are substantially brighter than V_{max} , implying significant spot coverage even at historical light maxima.

Our computed spot fractions represent the projected, limb-darkened spot coverages of the visible hemisphere. Figure 8 illustrates the range of possible values for the actual fractional photospheric spot coverage for a given measured f_s , computed from spherical geometry formulae. For example, $f_s = 20\%$ could correspond to as little as 5% actual coverage, if all the spot coverage is concentrated in a

TABLE 3
COMPUTED STARSPOT PROPERTIES

| Star | Date | Phase | D_{7055} | D_{8860} | Best-Fit f_s |
|--------------------|-------------|-------|------------|------------|----------------|
| EI Eri | 1989 Oct 9 | 0.52 | 0.009 | 0.004 | 0.17 |
| | 1989 Oct 11 | 0.53 | 0.012 | 0.006 | 0.22 |
| | 1989 Oct 13 | 0.53 | 0.015 | 0.004 | 0.29 |
| | 1989 Oct 14 | 0.05 | 0.010 | 0.000 | 0.20 |
| | 1990 Mar 15 | 0.07 | 0.024 | 0.011 | 0.36 |
| | 1990 Mar 18 | 0.61 | 0.026 | 0.012 | 0.38 |
| | 1991 Feb 6 | 0.69 | 0.008 | 0.003 | 0.15 |
| | 1994 Feb 6 | 0.20 | 0.016 | 0.004 | 0.29 |
| V1794 Cyg..... | 1989 Oct 9 | 0.59 | 0.016 | 0 | 0.29 |
| | 1989 Oct 10 | 0.88 | 0.018 | 0 | 0.32 |
| | 1989 Oct 11 | 0.24 | 0.008 | 0 | 0.16 |
| | 1989 Oct 12 | 0.52 | 0.017 | 0 | 0.30 |
| | 1989 Oct 13 | 0.81 | 0.018 | 0 | 0.32 |
| | 1992 Sep 12 | 0.91 | 0.018 | 0 | 0.32 |
| | 1992 Sep 14 | 0.53 | 0.023 | 0 | 0.37 |
| | 1992 Sep 15 | 0.78 | 0.020 | 0 | 0.34 |
| | 1992 Sep 16 | 0.13 | 0.012 | 0 | 0.23 |
| σ Gem | 1988 Mar 26 | 0.01 | 0.031 | 0 | 0.21 |
| | 1989 Mar 10 | 0.81 | 0 | 0 | 0 ^a |
| | 1989 Mar 12 | 0.90 | 0 | 0 | 0 ^a |
| | 1990 Mar 15 | 0.68 | 0.028 | 0 | 0.19 |
| | 1990 Mar 17 | 0.77 | 0.023 | ... | 0.14 |
| | 1990 Mar 18 | 0.83 | 0.027 | 0 | 0.18 |
| | 1990 Mar 19 | 0.88 | 0.027 | 0 | 0.18 |
| | 1990 Apr 10 | 0.01 | 0.036 | 0 | 0.26 |
| | 1990 Apr 11 | 0.06 | 0.033 | 0 | 0.23 |
| | 1990 Apr 12 | 0.10 | 0.037 | 0 | 0.26 |
| | 1990 Dec 17 | 0.82 | 0.023 | 0 | 0.14 |
| | 1991 Feb 6 | 0.41 | 0.045 | 0 | 0.33 |
| 1994 Feb 2 | 0.11 | 0.038 | 0 | 0.27 | |
| V1762 Cyg..... | 1989 Mar 12 | 0.04 | 0.032 | 0.016 | 0.24 |
| II Peg | 1989 Oct 9 | 0.17 | 0.048 | 0.031 | 0.43 |
| | 1989 Oct 10 | 0.32 | 0.050 | 0.039 | 0.47 |
| | 1989 Oct 12 | 0.62 | 0.062 | ... | 0.52 |
| | 1989 Oct 13 | 0.77 | 0.063 | 0.045 | 0.53 |
| | 1989 Oct 14 | 0.92 | 0.066 | 0.049 | 0.55 |
| | 1992 Sep 11 | 0.01 | 0.056 | 0.049 | 0.52 |
| | 1992 Sep 12 | 0.12 | 0.046 | 0.044 | 0.48 |
| | 1992 Sep 14 | 0.42 | 0.046 | 0.031 | 0.43 |
| 1992 Sep 15 | 0.56 | 0.052 | 0.036 | 0.47 | |
| 1992 Sep 16 | 0.73 | 0.066 | 0.055 | 0.56 | |

^a An apparent flare prevented the accurate measurement of TiO band depths on these dates.

^b No 8860 Å band observations were obtained on these dates.

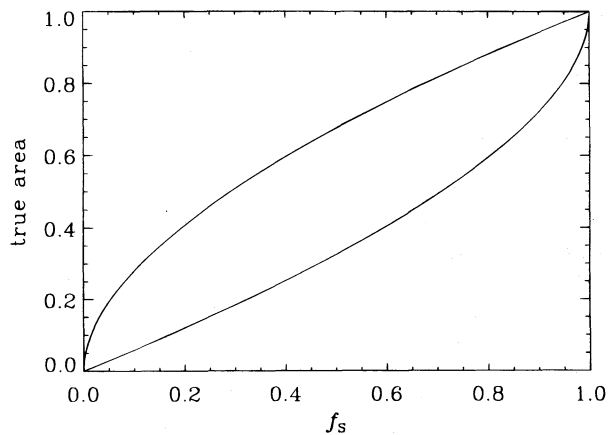


FIG. 8.—Illustration of the relationship between f_s (the projected, limb-darkened spot filling factor measured by our spectroscopic technique) and the actual fractional starspot coverage for two extreme cases: a single spot at disk center (*lower curve*), and a ring-shaped spot at the stellar limb (*upper curve*). For any given f_s measurement, the true spot area will lie between these two curves. A linear limb-darkening coefficient of $\epsilon = 0.6$ was assumed.

monolithic, circular region at disk center. On the other hand, the same f_s could correspond to as much as 33% actual coverage if the spot were in the shape of a ring along the star's limb. Since photometric measurements are similarly affected by limb-darkening and projection effects, the filling factor we calculate should always anticorrelate with the photometric brightness of the star.

4.5. Possible ΔT versus $\log g$ Relation

Plotting ΔT versus $\log g$ for our stars and including a point for the Sun at $\Delta T \approx 1800$ K [$T_S(\odot) \approx 4000$ K; e.g., Maltby et al. 1986] and $\log g = 4.4$, we find an increasing trend (Fig. 9; see also Saar, O'Neal, & Neff 1995). Here we have used a more refined estimate for II Peg, $\log g \approx 3.7$, based on $M/M_\odot \approx 1$, and $R/R_\odot \approx 2.2$ (Vogt 1981). A linear fit yields $\Delta T = 590 \log g - 680$ K ($\sigma = 240$ K); the data can also be fitted reasonably with $\Delta T = 220 \times g^{0.22}$ ($\sigma = 270$ K). We have compared our results with the photo-

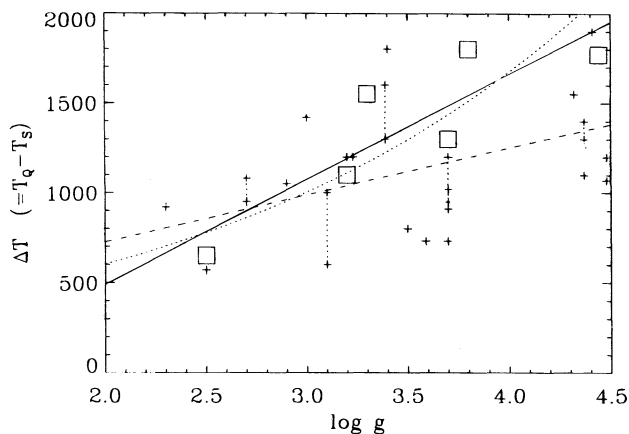


FIG. 9.—Relation between $\log g$ and $\Delta T \equiv T_Q - T_S$. Our TiO band results and the Sun are plotted as squares, with linear (*solid line*) and power-law (*dotted line*) fits shown. Compiled photometric results (*crosses*, with multiple T_S values connected) from Eaton (1992) show a weaker linear trend (*dashed line*).

metric ΔT values compiled by Eaton (1992) and $\log g$ estimates based on data in Schrijver & Zwaan (1991), Strassmeier et al. (1993), and Gray (1988). The photometric results also suggest that ΔT increases with $\log g$, but the trend is less clear, and it shows considerably more scatter and a shallower slope; the best linear fit is $\Delta T = 260 \log g + 200$ K ($\sigma = 340$ K).

If these relationships are real, they imply that the temperature contrast between spot and quiet photosphere is reduced in lower gravity stars. This might be the result of a changed pressure balance at the spot boundary. Horizontal pressure balance requires $\Delta P_{\text{gas}} = P_{\text{ext}} - P_{\text{int}} \approx B_S^2/8\pi$. If we take the stellar surface layers to be an adiabatic environment, $P_{\text{gas}} \propto T^{5/2}$, so that $\Delta P_{\text{gas}} \propto T^{3/2}\Delta T$. Using the approximate relation $P_{\text{gas}} \propto g^{2/3}$ (e.g., Gray 1992) and $\Delta P_{\text{gas}} \approx P_{\text{ext}}$ (for $P_{\text{ext}} \gg P_{\text{int}}$; Skumanich 1992), we then have $T^{3/2}\Delta T \propto g^{2/3}$, or $\Delta T \propto g^{4/15}$, very close to the $g^{0.22}$ relation we find in the data. One possible explanation for this is that mean starspot field strengths are smaller on low-gravity stars, reflecting the lower photospheric pressures with which they must be in horizontal pressure equilibrium (e.g., Skumanich 1992). Indirect support of this idea comes from the apparently small plage/network field strengths on evolved stars (Marcy & Bruning 1984; Saar 1990) and the low magnetic fluxes measured in dark regions of HR 1099 (Donati et al. 1992). The ΔT values may thus be indirect indicators of the trends of B_S values in stars.

4.6. Improving and Extending This Technique

There remain difficulties with our technique. These include the problems determining T_Q from spectroscopy alone, the difficulty obtaining accurate parameters for warmer spots (due to lack of 8860 Å band absorption), the inability to measure small f_s , and the ambiguity between f_s and the true, physical area coverage. We plan to address the first two of these by analyzing echelle spectra taken with the Penn State Fiber-Optic Echelle spectrograph at Kitt Peak, the QDSS Echelle at Penn State's Black Moshannon Observatory, and the SOFIN Echelle Spectrograph at the Nordic Optical Telescope. There are enough temperature diagnostics in these spectra to allow us to derive T_Q directly and to probe spot parameters on a much wider T_{eff} range of active stars. We will be able to measure smaller f_s values by observing in the infrared K band, where spots are substantially brighter relative to the unspotted photosphere than in the visual. Finally, by obtaining better phase coverage and using, e.g., a maximum-entropy inversion method, we should be able to determine a physical area starspot coverage. Our analysis could also provide a very useful additional constraint in Doppler imaging studies (O'Neal, Neff, & Saar 1995).

5. SUMMARY

We have analyzed TiO observations of five evolved single-lined active stars. Using the depths of the TiO bands at 7055 and 8860 Å, we have independently measured the areas and temperatures of the starspots on these active stars. We used contemporaneous photometry to compute the unspotted photospheric temperature.

In four epochs of observing EI Eri, we found $T_S = 3700 \pm 200$ K and f_s ranging from 17% to 38%. For II Peg, in two epochs of observation, we found $T_S = 3500 \pm 100$ K and f_s between 43% and 56% correlating with the visual

light curve. We observed V1762 Cyg on one night and determined $T_S = 3450$ K and $f_S = 24\%$.

V1794 Cyg and σ Gem have starspots too warm for us to uniquely determine their temperature, because they do not produce a measurable depth in the 8860 Å band. In both cases, contemporaneous photometry aids in estimating T_Q and T_S . Assuming $T_S = 3800$ K for V1794 Cyg, the spot filling factor varied from 16% to 37% in two epochs of observation. For σ Gem, taking $T_Q = 4500$ K and $T_S = 3850$ K, the maximum filling factor we observed was 33%.

For EI Eri, σ Gem, V1762 Cyg, and II Peg, we found substantially higher starspot filling factors than computed by other investigators using different techniques. Using our f_S values and contemporaneous photometry, we compute revised values of the immaculate V magnitude $V(f_S = 0)$ (see Table 2). For II Peg and V1794 Cyg, these values are substantially brighter than the historical maximum V magnitudes, implying that some starspot coverage is always present on these stars.

We find evidence for a correlation between $\Delta T (= T_Q - T_S)$ and $\log g$. We suggest that the relationship could be the result of lower starspot magnetic field strengths on active stars of lower gravity and the corresponding decrease in the pressure and temperature contrast between the photosphere and the umbra.

D. O. was supported by the NASA Space Grant College Fellowship Program. We thank Bob Dempsey, Lauri Jetsu, and Greg Henry for allowing us to use their unpublished photometry. We thank Sami Solanki for helpful discussions of sunspot structure, and L. Jetsu and the referee, K. Strassmeier, for insightful comments on the manuscript. The observations were obtained through the National Solar Observatory's Solar-Stellar Program, which we thank for generous observing time and support. This work was supported in part by NASA grant NAGW-2603 to The Pennsylvania State University. This work made use of the SIMBAD data base operated by CDS, Strasbourg, France.

REFERENCES

- Allard, F. 1990, Ph.D. thesis, Univ. of Heidelberg
 Böhm-Vitense, E. 1980, *ARA&A*, 19, 295
 Bopp, B. W., & Dempsey, R. C. 1989, *PASP*, 101, 516
 Byrne, P. B., et al. 1995, *A&A*, 299, 115
 Dempsey, R. C., Bopp, B. W., Henry, G. W., & Hall, D. S. 1993, *ApJS*, 86, 293
 Dempsey, R. C., Bopp, B. W., Strassmeier, K. G., Granados, A. F., Henry, G. W., & Hall D. S. 1992, *ApJ*, 392, 187
 Donati, J.-F., Brown, S. F., Semel, M., Rees, D. E., Dempsey, R. C., Matthews, J. M., Henry, G. W., & Hall, D. S. 1992, *A&A*, 265, 682
 Doyle, J. G., et al. 1992, *A&AS*, 96, 351
 Eaton, J. A. 1992, in *Surface Inhomogeneities on Late-Type Stars*, ed. P. B. Byrne & D. J. Mullan (Berlin: Springer), 15
 Feast, M. W. 1981, in *Physical Processes in Red Giant Stars*, ed. I. Iben, Jr., & A. Renzini (Dordrecht: Reidel), 193
 Fekel, F. C., Quigley, R., Gillies, K., & Africano, J. L. 1987, *AJ*, 94, 726
 Gray, D. F. 1988, *Lectures on Spectral Line Analysis: F, G, and K Stars* (Arva, Ontario: The Publisher)
 ———. 1992, *The Observation and Analysis of Stellar Photospheres* (Cambridge: Cambridge Univ. Press)
 Hackman, T., Piskunov, N. E., Poutanen, M., Strassmeier, K. G., & Tuominen, I. 1991, in *The Sun and Cool Stars: Activity, Magnetism, Dynamics*, ed. I. Tuominen, D. Moss, & G. Rüdiger (Berlin: Springer), 321
 Hatzes, A. P. 1993, *ApJ*, 410, 777
 Hatzes, A. P., & Vogt, S. S. 1992, *MNRAS*, 258, 387
 Henry, G. W., Eaton, J. A., Hamer, J., & Hall, D. S. 1995, *ApJS*, 97, 513
 Hoffleit, D., & Jaschek, C. 1982, *The Bright Star Catalogue* (4th ed.; New Haven: Yale Univ. Obs.)
 Huenemoerder, D. P. 1986, *AJ*, 92, 673
 Jetsu, L., Huovelin, J., Tuominen, I., Vilhu, O., Bopp, B. W., & Piirola, V. 1990, *A&A*, 236, 423
 Jetsu, L., Pelt, J., & Tuominen, I. 1993, *A&A*, 278, 449
 Kurucz, R. L. 1991, in *Precision Photometry: Astrophysics of the Galaxy*, ed. P. Davis, A. Uppgren, & K. Janes (Schenectady: L. Davis), 27
 Maltby, P., Avrett, E. H., Carlsson, M., Kjeldseth-Moe, O., Kurucz, R. L., & Loeser, R. 1986, *ApJ*, 306, 284
 Marcy, G. W., & Bruning, D. H. 1984, *ApJ*, 281, 286
 Neff, J. E., O'Neal, D., & Saar, S. H. 1995, *ApJ*, 452, 879 (Paper I)
 Olah, K., Panov, K. P., Pettersen, B. R., Valtaja, E., & Valtaja, L. 1989, *A&A*, 218, 192
 O'Neal, D., Neff, J. E., & Saar, S. H. 1995, in *IAU Symp. 176, Stellar Surface Structure*, Poster Proc., ed. K. Strassmeier (Vienna: Univ. of Vienna), 32
 Poe, C. H., & Eaton J. A. 1983, *BAAS*, 15, 877
 Ridgway, S. T., Joyce, R. R., White, N. M., & Wing, R. F. 1980, *ApJ*, 235, 126
 Rodonò, M., & Cutispoto, G. 1992, *A&AS*, 95, 55
 Saar, S. H. 1990, in *The Solar Photosphere: Structure, Convection, Magnetic Fields*, ed. J. O. Stenflo (Dordrecht: Kluwer), 427
 Saar, S. H., O'Neal, D., & Neff, J. E. 1995, in *IAU Symp. 176, Stellar Surface Structure*, Poster Proc., ed. K. Strassmeier (Vienna: Univ. of Vienna), 105
 Schrijver, C. J., & Zwaan, C. 1991, *A&A*, 251, 183
 Skumanich, A. 1992, in *Surface Inhomogeneities on Late-Type Stars*, ed. P. B. Byrne & D. J. Mullan (Berlin: Springer), 94
 Smith, M. A., & Giampapa, M. S. 1987, in *Cool Stars, Stellar Systems, and the Sun*, ed. J. Linsky & R. Stencel (Berlin: Springer), 477
 Smith, M. A., & Jaksha, D. 1984, in *Cool Stars, Stellar Systems, and the Sun*, ed. S. Baliunas & L. Hartmann (Berlin: Springer), 183
 Stauffer, J. R., & Hartmann, L. W. 1986, *ApJS*, 61, 531
 Strassmeier, K. G. 1990, *ApJ*, 348, 682
 Strassmeier, K. G., et al. 1988, *A&A*, 192, 135
 ———. 1991, *A&A*, 247, 130
 Strassmeier, K. G., Hall, D. S., Fekel, F. C., & Scheck, M. 1993, *A&AS*, 100, 173
 Strassmeier, K. G., Hall, D. S., & Henry, G. W. 1994, *A&A*, 282, 535
 Vogt, S. S. 1981, *ApJ*, 247, 975
 ———. 1988, in *The Impact of Very High S/N Spectroscopy on Stellar Physics*, ed. G. Cayrel de Strobel & M. Spite (Dordrecht: Kluwer), 253